Flexural Behavior of Steel–concrete–steel Sandwich Slabs

K. M. El-sayed[1], N. N. Khalil[1] and T. A. El Backlesh[1*]

[1]*Department of Civil Engineering, Benha Faculty of Engineering, Benha University, Egypt.*

Authors' contributions

This work was carried out in collaboration between all authors. All authors read and approved the final manuscript.

Original Research Article	

ABSTRACT

Aims: Study the flexural behavior of steel–concrete–steel sandwich slabs.
Methodology: Ten SCS slabs full scale specimens were prepared and experimentally tested taking into account the variables of this study.
Study Design: Parametric study is carried out by varying the thickness of (bottom & top) steel plates and types of shear connectors.
Results: The experimental results included ultimate load, vertical deflection at three points, slip between steel plate & concrete core and mode of failure.
Conclusion: Test results show that steel-concrete-steel slabs have good flexural characteristics. The failure modes observed during experiments were occurred due to shear studs rupture, concrete cracking and yielding of steel plates. The shear studs was found to be effective not only in ultimate load capacity but also in vertical deflection.

Keywords: SCS slabs; shear studs; ultimate load behavior and load carrying.

*Corresponding author: E-mail: tark.elbaklish@bhit.bu.edu.eg, totobeko631985@gmail.com;*

ABBREVIATIONS

B: width of plate; E: elastic modulus of steel; h_c: depth of concrete core; f_{cu}: Cubic strength of concrete; f_t: cylinder strength of concrete; L: length of slab; P_u: ultimate load applied on a slab; S_x: longitudinal spacing of shear studs; S_y: transverse spacing of shear studs; t_b: thickness of bottom plate; t_p: thickness of top plate; Δ_o: deflection at mid-point for yield load; Δ_u: deflection at mid-point for ultimate load.
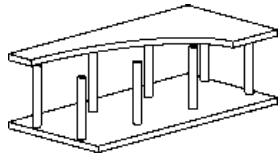
1. INTRODUCTION

The need for large construction with higher specific strength and stiffness is increasing. This is found in structures such as ships, Train stations and high towers where are interest in increasing the load capacity to structure weight ratio. To deliver such structures, engineers can either find a new structural material or produce a new structural topology. In civil engineering applications, steel-concrete-steel (SCS) sandwich construction has been developed using the sandwich structure concept. It is a combination of steel and concrete materials.

The SCS sandwich construction consists of two steel plates and concrete core that are connected together by mean of series shear connectors. The state-of-the-art construction forms of the SCS sandwich structures are double-skin sandwich construction (DSC) and Bi-Steel sandwich construction (Bi-Steel). They are different only due to the pattern of their shear connectors, as shown in Fig. 1.
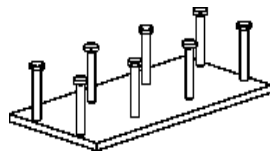
(a) Double-skin sandwich construction (DSC)

(b) Bi-steel sandwich construction (Bi-steel)

Fig. 1. The state-of-the-art construction forms of the SCS sandwich structures

Being an alternative construction technique, the SCS was introduced for the Conwy River submerged-tube-tunnel crossing project in the mid-1980s. It is difficult to make reinforced concrete structure watertight, so the external

steel plates provide water tightness. Although the DSC is similar to steel-concrete composite construction, but it was not qualified for this project due to the difficulties of on-site construction, especially the depth control of the sandwich core.

In 2002, the research to understanding the Behavior of double skin composite construction was conducted by B. McKinley and L. F. Boswell [1]. In this paper the preliminary test results using 16 large-scale, simply supported, three-point bending tests to study the elastic and plastic behavior of this specimens. For result, there is no difference in the elastic and early plastic deformations and load characteristics. Due to the continuity of the steel in Bi-Steel, it was evident that this construction could withstand larger deformations before failure. Failure of the two different types of construction was different. The studded specimens failed by studs (attached to the compression plate) pulling out of the concrete, whereas the Bi-Steel specimens failed through local buckling of the compression plate.

In 2005, the experimental study to obtain the static behavior of eighteen Bi-Steel beams was reported by M. Xie, N. Foundoukos, J.C. Chapman [2,3]. Eighteen beams having a range of span, depth, plate thickness and bar spacing, have been tested under static loading. The beams were 400 mm wide with two rows of both ended friction-welded bar connectors in the transverse direction and the concrete core was the ready-mix concrete of grade C40/50. The failure modes of beams subjected to the static load were observed and reported as a tension plate failure, a bar tension failure, a bar shear failure, and a concrete shear failure. The tests confirm that for ductile failure, beams should be designed to fail by yielding of the tension plate.

The Bi-Steel form get over some of the existing on site construction problems of the SCS, both ends of a shear connector can be jointly fixed to the steel face plates. It seems to be an advantageous solution as a simplified low-cost-construction technique because it just requires simplified construction tools that are now generally available at the construction site. The

SCS sandwich construction with the innovative J-J hook connectors [4-6]. Considering the existing construction forms of Bi-Steel structures, it may be seen that all of the current types of shear connector are similar in alignment pattern. They all align in the vertical direction, the axis of shear connector is normal to the face plates. However, it is known that a concrete filled Bi-Steel sandwich slab under bending load suffers diagonal shear cracks.

2. EXPERIMENTAL INVESTIGATION

2.1 Details of Test Specimens

Ten SCS slabs, all having same cross-section and span dimension (160*30*15 cm) were tested to failure. They were simply supported over a span of 145 cm on two side. No conventional reinforcement in the form of reinforcement bar was provided in any of the slabs, which enabled the performance of shear connectors to be studies exclusively. Of the five specimens identified in the text as DSC 4-4-S1 to DSC 4-4-S5 and the other five specimens identified in the text as DSC 6-6-S1 to DSC 6-6-S5. Five specimens DSC 4-4-S1 to DSC 4-4-S5 were fabricated with top and bottom plates of equal thickness of 4 mm. The remaining five specimens DSC 6-6-S1 to DSC 6-6-S5 were fabricated with top and bottom plates of equal thickness of 6 mm. Stud spacing in each of these specimens were fixed in all specimens, where S_x =10 cm and S_y = 15 cm, as shown in Fig. 2.

The ten specimens have a different shear connectors. The shear studs in form of plates were installed in order to the long dimension of its x-section was perpendicular to the longitudinal axis of specimen. The details of all the test specimens are summarized in Table 1.
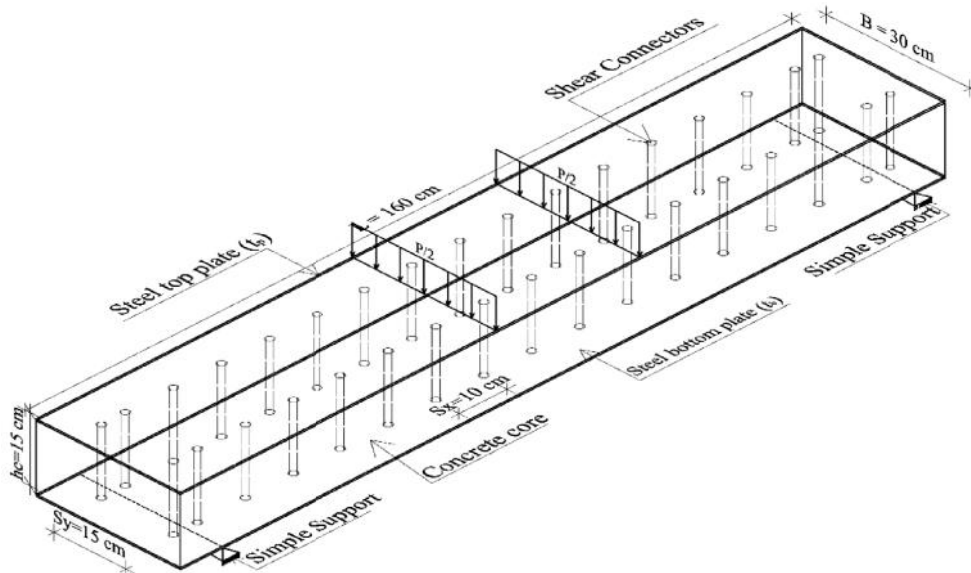

Fig. 2. A typical layout of studs and the relevant details of specimens

Table 1. Details of test specimens

| Specimen	$t_{p\,(mm)}$	$t_{b(mm)}$	$h_{c(cm)}$	Type of shear studs
DSC 4-4-S1	4.0	4.0	15	Bars of 10 mm diam.
DSC 4-4-S2	4.0	4.0	15	Bars of 16 mm diam.
DSC 4-4-S3	4.0	4.0	15	Plates of 5*40 mm x-sec
DSC 4-4-S4	4.0	4.0	15	Plates of 10*20 mm x-sec
DSC 4-4-S5	4.0	4.0	15	Bolts of 16 mm diam.
DSC 6-6-S1	6.0	6.0	15	Bars of 10 mm diam.
DSC 6-6-S2	6.0	6.0	15	Bars of 16 mm diam.
DSC 6-6-S3	6.0	6.0	15	Plates of 5*40 mm x-sec
DSC 6-6-S4	6.0	6.0	15	Plates of 10*20 mm x-sec
DSC 6-6-S5	6.0	6.0	15	Bolts of 16 mm diam.
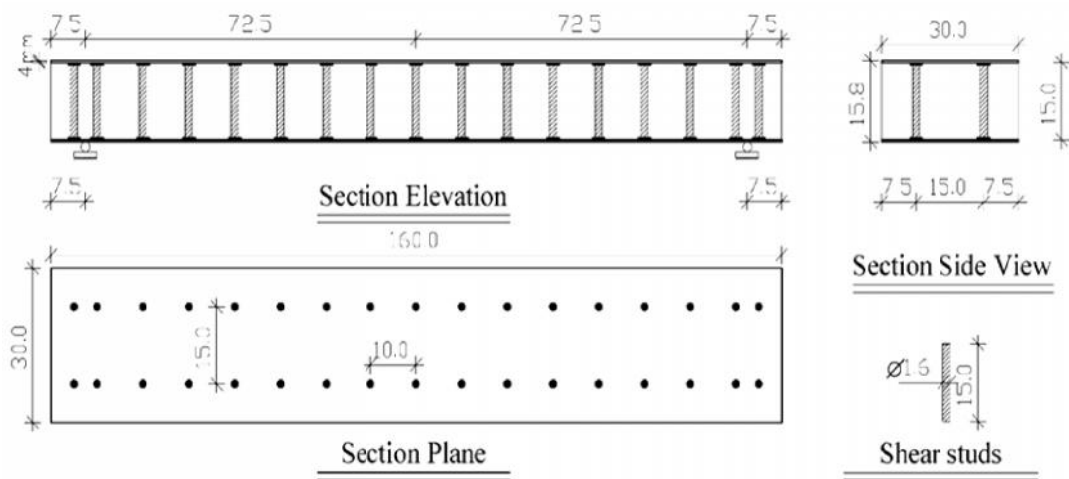
Fig. 3. A typical layout of studs and the relevant details of DSC 4-4-S2

Fig. 4. Formwork in vertical position for concrete pouring

2.2 Preparation of Test Specimens

Hot rolled steel plates of Grade 37A were cut to the required dimensions. Many types of shear connectors were used with gross length of 15 cm, then they were welded at specified spacing of 10 cm to both side of steel plates. A typical layout of studs and relevant details are show in Fig. 3 above. The studs were welded using electric arc. For this type of slabs, a strong formwork is not needed because they are act as a formwork. Concrete was poured to with the formwork in vertical position as show in Fig. 4 above. Micro-concrete having maximum aggregate size 10 mm was mixed in the laboratory using tilting type drum mixer. Fresh concrete was poured through the specimen, and extreme care was taken to achieve sufficient compaction of concrete in the regions of studs and at corners. For DSC specimens, nine cubes (100 mm) and six cylinders (100 mm diameter × 200 mm length) were poured and compacted from the same mix. The formwork was removed gently without allowing any damage to the composite specimen. The outside plate surface was cleaned at the mid span zone to the upper and lower plates, 20 mm long strain gauges was fixed.

3. MATERIAL PROPERTIES

3.1 Concrete

The concrete consisted of ordinary Portland cement, siliceous sand and a crushed stone course as an aggregate of 10 mm maximum size. A recommended concrete mixture is as follows: 400 Kg of Portland cement to 0.50 cubic meter of sand to 0.7 cubic meter of gravel. For moderately moist sand and gravel (the usual condition) was used, then the amount of water to be added should be approximately 170 liters per cubic meter of concrete [7]. Trial mixes were used to determine a suitable mix design. The properties of concrete specimens were determine from nine cubes and six cylinders tests. Development of concrete strength was observed closely by testing the cubes and cylinders after 7 and 28 days. The average value of compressive strength obtained from cube tests is f_{cu} = 32 N/mm^2. Splitting tensile strength form cylinders tests is f_t = 3.3 N/mm^2.

4

Table 2. Mechanical properties of steel plates

| Modulus of elasticity (E) (N/mm²)	Yield stress (f_y) (N/mm²)	Ultimate tensile strength (f_u) (N/mm²)	Yield strain (ε_y) %	Strain at ultimate tensile strength (ε_u) %
208,900	246	365	0.50	3.5

3.2 Steel Plates

The tensile properties of steel plates were determined in accordance with ASTM procedure. Three tension tests coupons for each of the test specimens were prepared as per ASTM E8/E8M-09 specification and they were cut from the same patch of the steel plates [8-10]. The Mechanical properties are given in Table 2.

4. TEST PROCEDURE

The DSC slabs to be tested was placed on two supports (hinged and roller support). Care was taken to ensure that the specimen was correctly positioned in the test frame and the center of the slab was in the line with the center of the loading head of the jack. The load was applied to the specimen by using a hydraulic jack of 100-ton capacity. A load cell of 100 ton capacity were used to measure the applied load. Deflections were measured using Linear Variable Deformation Transducers (LVDT) located at the center and under the two points load. The end slip between steel plates and concrete was measured at the end of steel plate and concrete

core, as show in Fig. 5. Before specimen loading, all strain gauges, load cell and LVDTs were connected to a data acquisition system which was programmed to record the output data. Then a small load (not exceeding 5 percent of the expecting ultimate load) was applied slowly and removed in order to eliminate any slack in the support system so that the specimen would be properly placed on the supports. This also helped to check the load cell, strain gauge and LVDTs properly.

During loading, the readings were observed and automatically recorded. The specimen was loaded every 150 kN more or less until to failure load. Close observation was made to locate the first crack, and the corresponding load was noted. Yielding in steel plates were carefully observed in order to obtain the corresponding load to the first yield. The ultimate load and the failure mode for each of the test specimens were noted and concrete cracking was marked. The test procedures adopted for all the specimens were the same. The slip between concrete and steel plates was measured for all specimens.
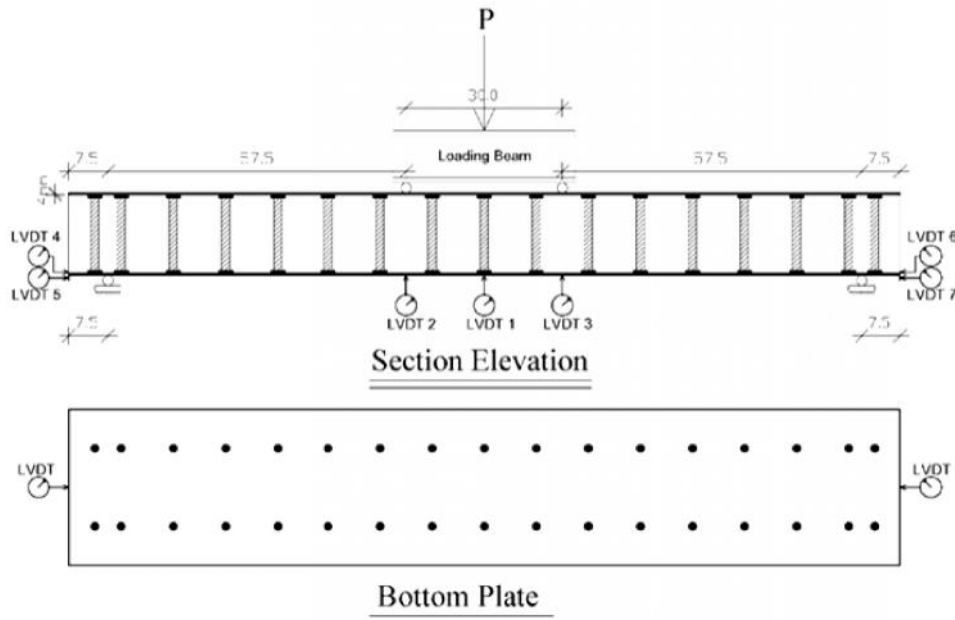

Fig. 5. The arranged of LVTDs

5. RESULTS AND DISCUSSION

The DSC specimens, for different plate thickness and different types of shear stud, were found to display various failure modes as listed below.

5.1 Concrete Cracking

Two types of cracks were observed. The first type occurred due to tensile stresses at the bottom side of the specimen, especially at mid span, as show in Fig. 6-a. The second type occurred due to the mutual pressure between steel studs and concrete which causes a longitudinal splitting cracks of concrete at the studs line, as show in Fig. 6-b. For all tested specimens, both cracking types were observed. However, the first type was noted firstly then the second type was observed suddenly at failure.
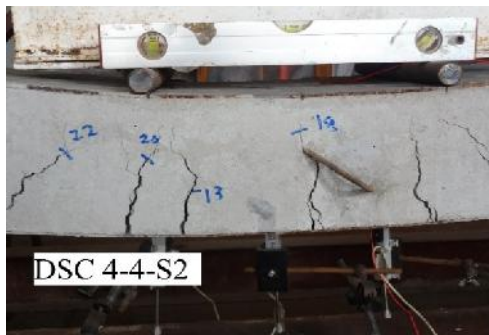
(a) Wide flexural crack in concrete core

(b) Splitting cracks in concrete core

Fig. 6. Mode of concrete cracking for specimen DCS 4-4-S2

The specimens DSC 4-4-S3 and DSC 6-6-S3 revealed a narrow cracks -on both side- relative to the rest of specimens as shown in Fig. 9 and Fig. 14 respectively. The large projected area of steel studs (5*40 mm) of specimens DSC 4-4-S3

and DSC 6-6-S3 produced lesser pressure on concrete compared to the other steel studs, consequently narrow cracks were generated as mentioned.

5.2 Failure of Shear Studs

Breaking of shear studs was followed by loud sound heard during testing. This failure was observed for specimens DSC 4-4-S1 and DSC 6-6-S1. The studs welded near to mid-span were found to be intact while those near to the edges were found to have a clear deformation before breaking off.

5.3 Yielding of Steel Plates

For all specimens, the stress at mid span of bottom steel plates reached to the yield stress at failure. The yielding started from the mid-point and spread rapidly outwards. Plate rupture did not occur, but very high strains in steel plates followed by concrete cracking and studs rupture was occurred.

The measured test results for the ten specimens are summarized in Table 3. Load-deflection Plots are given in Fig. 7.a and Fig. 7.b for plates of 4 mm and 6 mm thickness, respectively.

It can be seen from Fig. 7 that load-deflection curve deviates from linear behavior after the beginning of steel plates yielding in most cases. For specimen DSC 4-4-S1, the first sign of crack appeared in the concrete when the load reached to 50 KN. A loud sound was heard indicating the breaking of shear studs when the load reached to 172 kN. After maximum load was reached, a load reduction was observed in load-deflection curve. Strain results at the mid span showed that yielding of bottom plate started when the load reached to 138 kN.

Specimen DSC 4-4-S2 compared to DSC 6-6-S2 had showed a softer behavior which is expected, at a load of 50 kN, the first sign of cracking appeared in the concrete at the mid span, then the crack were propagated and the load-deflection curve became even more flat and continued till the load failure is reached at 228 kN and deflection recorder 57 mm. The tension cracks at mid span and splitting cracks at the ends are shown in Figs. 8a and 8b, respectively. Wide cracks in the concrete at the supports indicated the presence a high pressure on concrete. 28 mm slip was observed between bottom plate and concrete at the ends.

Table 3. Summary of the test results

Specimens	Yield load P_y (kN)	1st crack load P_{ck}(kN)	Ultimate load P_u (kN)	Δ_o (mm)	Δ_u (mm)	ε (P_u) µm/m	Slip (mm)
DSC 4-4-S1	138	50	172	8.9	12.68	1994	18.9
DSC 4-4-S2	187	50	228	7.46	57.56	31304	12.8
DSC 4-4-S3	221	50	260	11	50.65	22884	18.93
DSC 4-4-S4	168	50	229	9.96	52.58	21884	24.12
DSC 4-4-S5	175	50	198	30.29	51.2	2335	7.1
DSC 6-6-S1	132	80	188	5.32	9.28	1291	11.19
DSC 6-6-S2	200	80	243	8.83	32.84	12789	9.2
DSC 6-6-S3	226	80	276	9.45	45.3	30307	16.3
DSC 6-6-S4	200	80	246	8.83	34.92	20451	22.3
DSC 6-6-S5	144	80	215	8.3	48.78	9921	7.8
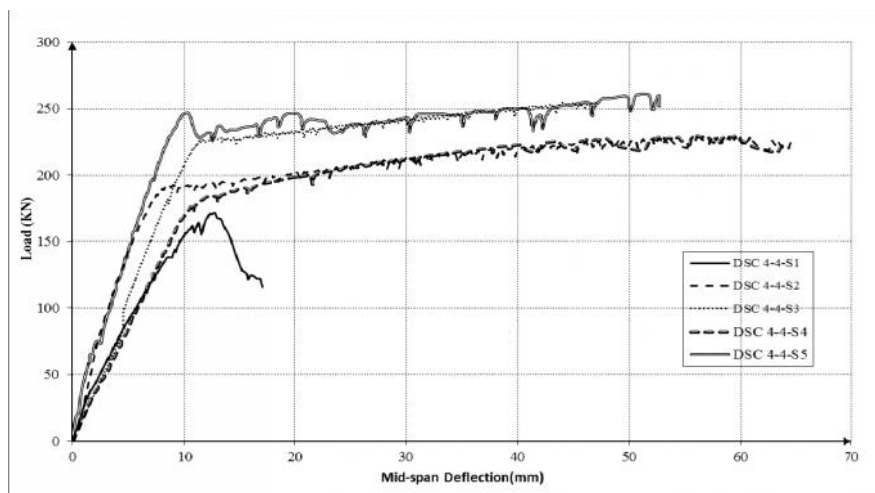
(a) Load -deflection curves for (DSC 4-4) series experimental test results
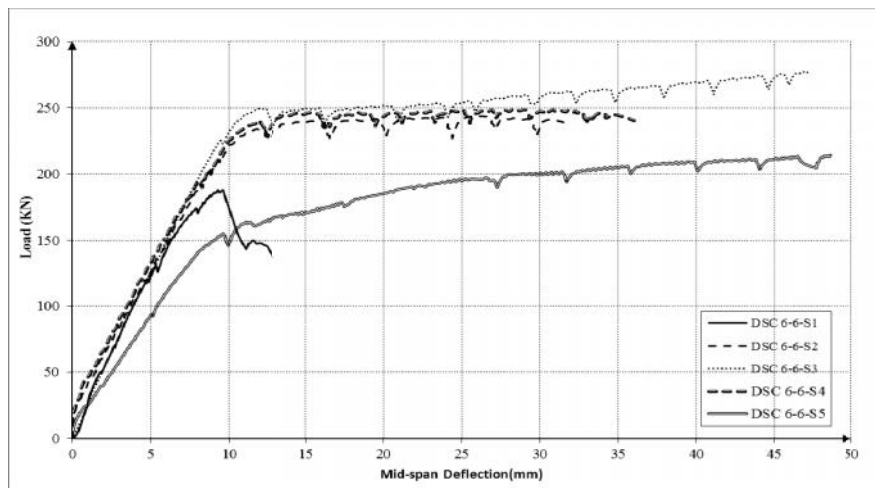
(b) Load -deflection curves for (DSC 6-6) series experimental test results

Fig. 7. Load-deflection plot for all the tested specimens

For DSC 4-4-S3, the first crack appeared in concrete when the load reached to 50 kN. Small cracks appeared in the concrete at many location of mid span, then the load-deflection curve became even more flat and continued till the load failure is reached at 260 kN and the deflection was 50 mm. The tension cracks at mid span and splitting cracks at the ends are shown in Fig. 9a and 9b, however these cracks were relatively narrow due to the low mutual pressure between concrete and steel studs as mentioned before.

For DSC 4-4-S4, the first crack appeared in concrete when the load reached to 50 kN. Cracks appeared in the concrete at many locations of mid span then the load-deflection curve became even more flat and continued till the load failure is reached at 229 kN and the deflection was 52 mm. Splitting in concrete was also observed indicating that concentrated pressure on concrete form shear studs, as show in Fig. 10a and 10b.

(a)   (b)

Fig. 8. View after failure load of the specimen DSC 4-4-S2 with wide crack in concrete (a), and close up view of the right side corner showing longitudinal cracks in concrete (b)
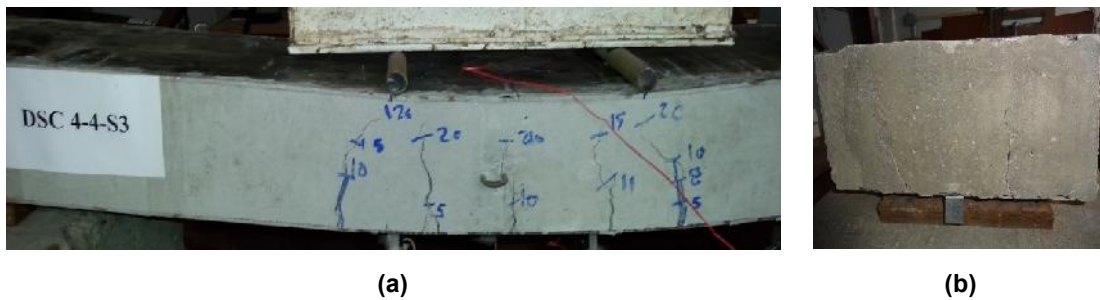

(a)   (b)

Fig. 9. View after failure load of the specimen DSC 4-4-S3 with wide crack in concrete (a), and close up view of the right side corner showing longitudinal cracks in concrete (b)

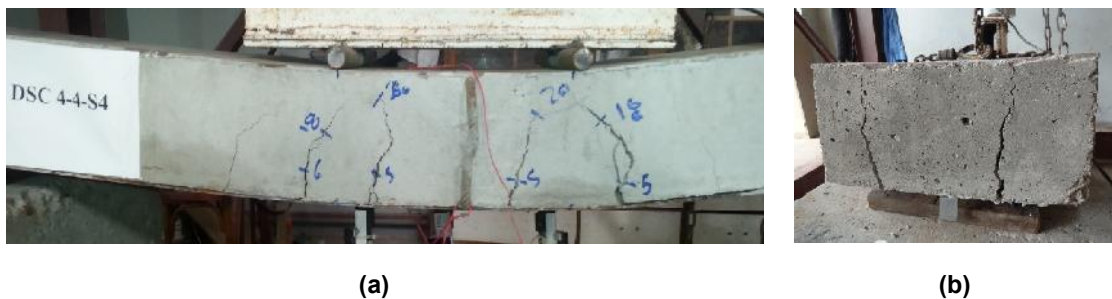

(a)   (b)

Fig. 10. View after failure load of the specimen DSC 4-4-S4 with wide crack in concrete (a), and close up view of the right side corner showing longitudinal cracks in concrete (b)

For DSC 4-4-S5, the first crack appeared in concrete when the load reached to 50 kN. Cracks appeared in the concrete at many locations of mid span then the load-deflection curve became even more flat and continued till the load failure is reached at 198 kN and the deflection was 51 mm, as show in Fig. 11a and 11b.

For DSC 6-6-S1, the first sign of crack appeared in the concrete when the load reached to 80 KN. A loud sound was heard indicating the breaking of shear studs when the load reached to 188 kN. After maximum load was reached, a load reducer was observed in load-deflection curve. Strain

results at the mid span showed that yielding of bottom plate started when the load reached to 132 kN, as show in Fig. 12a and 12b.

For DSC 6-6-S2, the first sign of cracking appeared in the concrete at the mid span, then the crack were propagated and the load-deflection curve became even more flat and continued till the load failure is reached at 243 kN and deflection recorder 33 mm. Wide cracks in the concrete at the supports indicated the presence a huge pressure on concrete. 16.3 mm slip was observed between bottom plate and concrete at the ends, as show in Fig. 13a and 13b.

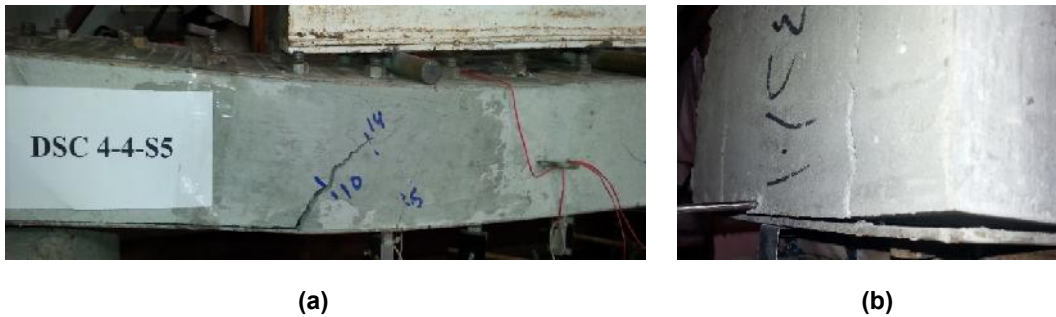
(a)   (b)

Fig. 11. View after failure load of the specimen DSC 4-4-S5 with wide crack in concrete (a), and close up view of the right side corner showing longitudinal cracks in concrete (b)

(a)   (b)

Fig. 12. View after failure load of the specimen DSC 6-6-S1 with wide crack in concrete (a), and close up view of the right side corner showing longitudinal cracks in concrete (b)

(a)   (b)

Fig. 13. View after failure load of the specimen DSC 6-6-S2 with wide crack in concrete (a), and close up view of the right side corner showing longitudinal cracks in concrete (b)

For DSC 6-6-S3, the first crack appeared in concrete when the load reached to 80 kN. Small cracks appeared in the concrete at many location of mid span, then the load-deflection curve became even more flat and continued till the load failure is reached at 276 kN and the deflection was 45 mm. The tension cracks at mid span and splitting cracks at the ends are shown in Fig. 14a and 14b, however these cracks were relatively narrow due to the low mutual pressure between concrete and steel studs as mentioned before.

For DSC 6-6-S4, the first crack appeared in concrete when the load reached to 80 kN. Cracks appeared in the concrete at many locations of mid span then the load-deflection curve became even more flat and continued till the load failure is reached at 246 kN and the deflection was 35 mm. Splitting in concrete was also observed indicating that concentrated pressure on concrete form shear studs, as show in Fig. 15a and 15b.

For DSC 6-6-S5, the first crack appeared in concrete when the load reached to 80 kN. Cracks appeared in the concrete at many locations of mid span then the load-deflection curve became even more flat and continued till the load failure is reached at 215 kN and the deflection was 49 mm ,as show in Fig. 16a and 16b.

(a)   (b)

Fig. 14. View after failure load of the specimen DSC 6-6-S3 with wide crack in concrete (a), and close up view of the right corner showing slide between concrete and steel plate (b)

(a)   (b)

Fig. 15. View after failure load of the specimen DSC 6-6-S4 with wide crack in concrete (a), and close up view of the right side corner showing longitudinal cracks in concrete (b)

(a)   (b)

Fig. 16. View after failure load of the specimen DSC 6-6-S5 with wide crack in concrete (a), and close up view of the right side corner showing longitudinal cracks in concrete (b)

6. PARAMETRIC STUDY

Parameter considered in this study are thickness of steel plates and type of shear studs. The effect of these parameters on ultimate load, strain, deflection and failure mode are obtained.

6.1 Thickness of Steel Plates

For all shear studs types, using steel plates of 6 mm thickness led to increase the ultimate load capacity by a range from 6.15% to 9.3% compared to specimens with 4 mm thickness, as show in Fig. 17.

For shear studs (S1, S3 and S5) using steel plates of 6 mm thickness led to reduce the mid span deflection by a range from 4.7% to 26% compared to specimens with 4 mm thickness, as

show in Fig. 18. However, higher reducer in mid span deflection ranged from 33% to 43% was obtained for specimens with shear studs S2 and S4.

6.2 Aspect Ratio of Shear Connectors

The aspect ratio of the cross sectional area of shear studs varied to study its effect on the structural behavior of tested specimen. Three values (1, 2 and 8) were used which correspond to shear studs (S1, S2 and S5), (S4) and (S3), respectively.

A significant effect of aspect ratio was observed on the ultimate load capacity y and mid span deflection, as show in Fig. 19 and Fig. 20, respectively.
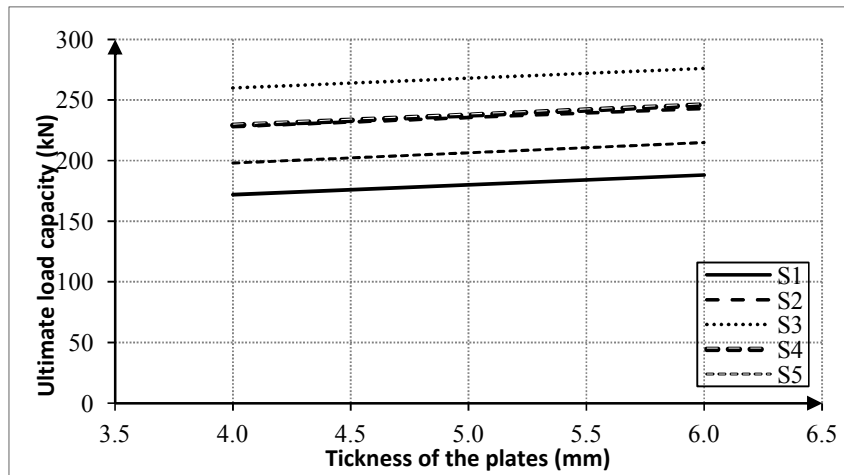

Fig. 17. Effect of steel plate thickness and shear connector type on ultimate load capacity
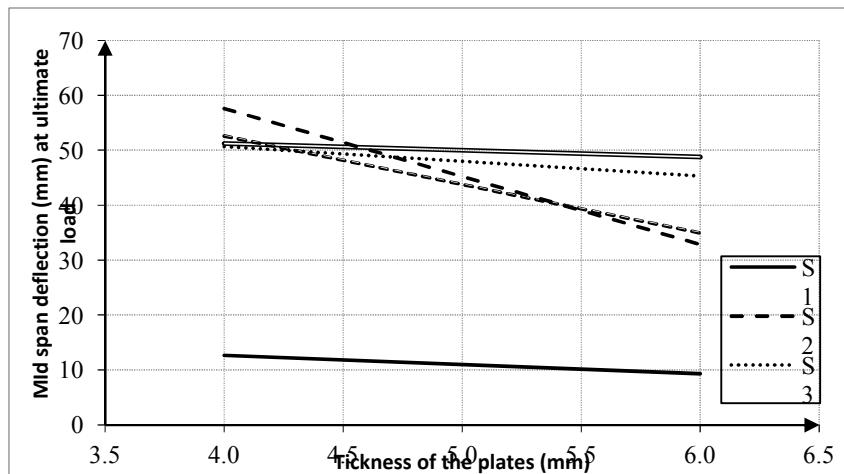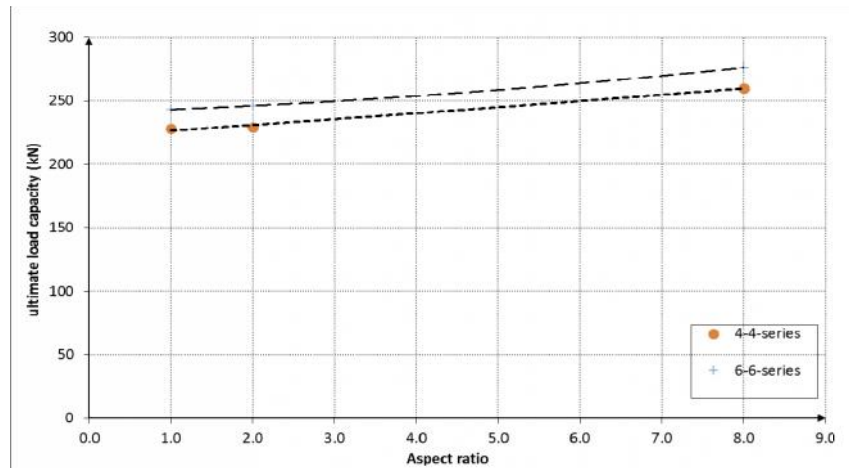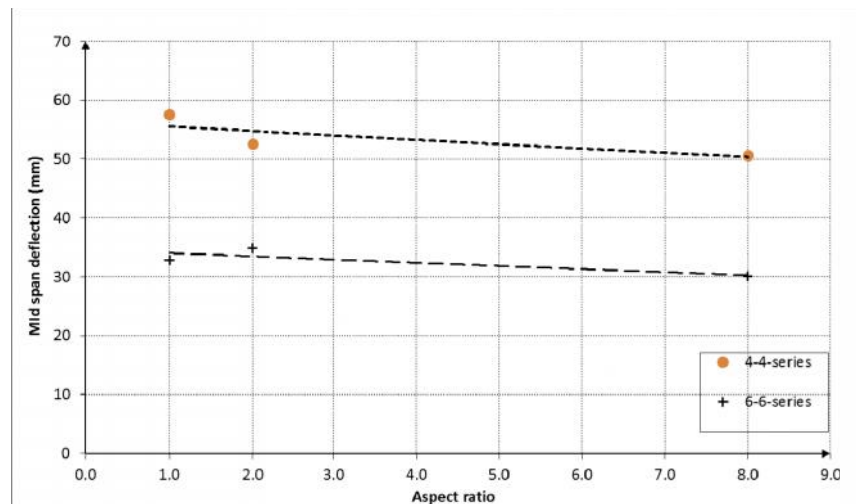

Fig. 18. Effect of steel plate thickness and shear connector type on the mid span deflection at ultimate load

Fig. 19. Effect of steel studs aspect ratio on the ultimate load capacity

Fig. 20. Effect of steel studs aspect ratio on the mid span deflection at ultimate load

Increasing the aspect ratio from 1 to 8 led to increase the ultimate load capacity by 14% and 13.6% for specimens of 4 mm and 6 mm steel plate thickness, respectively.

When the aspect ratio increase from 1 to 8, the mid span deflection were reduced by 12.2% and 14.1% for 4 mm and 6 mm steel plate thickness, respectively. Increasing the aspect ratio produces lower pressure on concrete. So, the specimens DSC 4-4-S3 and DSC 6-6-S3 are more resistant and rigid.

6.3 Cross Section of Shear Connectors

For the same plate thickness, as seen in Figs. 14 and 15, it can be observed that ultimate load capacity increase with increasing in cross section form 0.785 cm2 to 2.01 cm2 by 32% as from DSC 4-4-S1 to DSC 4-4-S2 and increase by 29% as from DSC 6-6-S1 to DSC 6-6-S2. Otherwise, it can observed that cross section of connector less than 1 cm2 is found to have negligible effect on mid span deflection response.

7. CONCLUSIONS

Test results show that steel-concrete-steel slabs have good flexural characteristics. The failure modes observed during experiments were occurred due to shear studs rupture, concrete cracking and yielding of steel plates. The shear studs was found to be effective not only in ultimate load capacity but also in vertical deflection.

The measured load vs. deflection curves confirm that yielding of the tension plates are the most occurred failure mode.

It can be observed that ultimate load capacity increase with increase in plate thickness. Using steel plates of 6 mm thickness led to increase the ultimate load capacity by a range from 6.15% to 9.3% compared to specimens with 4 mm thickness.

It can be observed that ultimate load capacity increase with increase in aspect ratio of the cross sectional area of shear studs. Increasing the aspect ratio from 1 to 8 led to increase the ultimate load capacity by 14% and 13.6% for specimens of 4 mm and 6 mm steel plate thickness, respectively. However, the mid span deflection decreased with the increasing in aspect ratio of the cross sectional area of shear studs. The mid span deflection were reduced by 12.2% and 14.1% for 4 mm and 6 mm steel plate thickness, respectively.

It can be observed that the mid span deflection decreased with the increasing in plate thickness. For shear studs (S1, S3 and S5) using steel plates of 6 mm thickness led to reduce the mid span deflection by a range from 4.7% to 26% compared to specimens with 4 mm thickness. However, higher reduction in mid span deflection ranged from 33% to 43% was obtained for specimens with shear studs S2 and S4, when the steel plate thickness was increased from 4 mm to 6 mm.

ACKNOWLEDGEMENTS

COMPETING INTERESTS

Authors have declared that no competing interests exist.

REFERENCES

1. McKinley B, Boswell LF. Behaviour of double skin composite construction. Journal of Constructional Steel Research. 2002;58(10):1347-1359.

2. Xie M, Foundoukos N, Chapman JC. Experimental and numerical investigation on the shear behavior of friction-welded bar-plate connections embedded in concrete. Journal of Constructional Steel Research. 2005;61(5):625–649.

3. Xie M, Chapman JC. Static and fatigue tensile strength of friction-welded bar-plate connections embedded in concrete. Journal of Constructional Steel Research. 2005;61(5):651-673.

4. Liew JYR, Sohel KMA. Lightweight steel–concrete–steel sandwich system with J-hook connectors. Engineering Structures. 2009;31(5):1166-1178.

5. Bowerman HG, Gough MS, King CM. Bi-steel design and construction guide. British Steel Ltd, Scunthorpe, London; 1999.

6. Bowerman H, Coyle N, Chapman JC. An innovative steel/concrete construction system. The Structural Engineer. 2002; 80(20):33-38.

7. European Committee for Standardization. Design of concrete structures and Euro code 2, Brussels; 1992

8. Lee PG, Shim CS, Chang SP. Static and fatigue behavior of large stud shear connectors for steel-concrete composite bridges. Journal of Constructional Steel Research. 2005;61(9):1270–1285.

9. Xuexin D. Fatigue analysis and design of steel-concrete-steel sandwich composite structures. PhD thesis, National University of Singapore; 2009.

10. Liew JYR, Sohel KMA. Structural performance of steel-concrete-steel sandwich composite structures. Advances in Structural Engineering. 2010;13(3):453-470.

Peer-review history:
The peer review history for this paper can be accessed here:
http://sciencedomain.org/review-history/16262